AMERICAN SOCIETY FOR MICROBIOLOGY | Journal of Virology®

VIRUS-CELL INTERACTIONS

Species-Specific Valid Ternary Interactions of HIV-1 Env-gp120, CD4, and CCR5 as Revealed by an Adaptive Single-Amino Acid Substitution at the V3 Loop Tip

Takaaki Koma,[a] Masaru Yokoyama,[b] Osamu Kotani,[b] Naoya Doi,[a] Nina Nakanishi,[a] Hayato Okubo,[a] Shun Adachi,[c] Akio Adachi,[c] Hironori Sato,[b] Masako Nomaguchi[a]

[a]Department of Microbiology, Tokushima University Graduate School of Biomedical Sciences, Tokushima, Tokushima, Japan
[b]Laboratory of Viral Genomics, Pathogen Genomics Center, National Institute of Infectious Diseases, Musashimurayama, Tokyo, Japan
[c]Department of Microbiology, Kansai Medical University, Hirakata, Osaka, Japan

Takaaki Koma and Masaru Yokoyama contributed equally to this work. The author order was decided based on the amount and importance of the contributions to the manuscript.

ABSTRACT Molecular interactions of the variable envelope gp120 subunit of HIV-1 with two cellular receptors are the first step of viral infection, thereby playing pivotal roles in determining viral infectivity and cell tropism. However, the underlying regulatory mechanisms for interactions under gp120 spontaneous variations largely remain unknown. Here, we show an allosteric mechanism in which a single gp120 mutation remotely controls the ternary interactions between gp120 and its receptors for the switch of viral cell tropism. Virological analyses showed that a G310R substitution at the tip of the gp120 V3 loop selectively abolished the viral replication ability in human cells, despite evoking enhancement of viral replication in macaque cells. Molecular dynamics (MD) simulations predicted that the G310R substitution at a site away from the CD4 interaction site selectively impeded the binding ability of gp120 to human CD4. Consistently, virions with the G310R substitution exhibited a reduced binding ability to human lymphocyte cells. Furthermore, the G310R substitution influenced the gp120-CCR5 interaction in a CCR5-type dependent manner as assessed by MD simulations and an infectivity assay using exogenously expressed CCR5s. Interestingly, an I198M mutation in human CCR5 restored the infectivity of the G310R virus in human cells. Finally, MD simulation predicted amino acid interplays that physically connect the V3 loop and gp120 elements for the CD4 and CCR5 interactions. Collectively, these results suggest that the V3 loop tip is a *cis*-allosteric regulator that remotely controls intra- and intermolecular interactions of HIV-1 gp120 for balancing ternary interactions with CD4 and CCR5.

IMPORTANCE Understanding the molecular bases for viral entry into cells will lead to the elucidation of one of the major viral survival strategies, and thus to the development of new effective antiviral measures. As shown recently, HIV-1 is highly mutable and adaptable in growth-restrictive cells, such as those of macaque origin. HIV-1 initiates its infection by sequential interactions of Env-gp120 with two cell surface receptors, CD4 and CCR5. A recent epoch-making structural study has disclosed that CD4-induced conformation of gp120 is stabilized upon binding of CCR5 to the CD4-gp120 complex, whereas the biological significance of this remains totally unknown. Here, from a series of mutations found in our extensive studies, we identified a single-amino acid adaptive mutation at the V3 loop tip of Env-gp120 critical for its interaction with both CD4 and CCR5 in a host cell species-specific way. This remarkable finding could certainly provoke and accelerate studies to precisely clarify the HIV-1 entry mechanism.

KEYWORDS HIV-1, Env-gp120, CD4, CCR5, V3 loop, adaptive mutation, species specificity, *in silico* structural analysis

Citation Koma T, Yokoyama M, Kotani O, Doi N, Nakanishi N, Okubo H, Adachi S, Adachi A, Sato H, Nomaguchi M. 2021. Species-specific valid ternary interactions of HIV-1 Env-gp120, CD4, and CCR5 as revealed by an adaptive single-amino acid substitution at the V3 loop tip. J Virol 95:e02177-20. https://doi.org/10.1128/JVI.02177-20.

Editor Viviana Simon, Icahn School of Medicine at Mount Sinai

Address correspondence to Hironori Sato, hirosato@nih.go.jp, or Masako Nomaguchi, nomaguchi@tokushima-u.ac.jp.

Received 11 November 2020
Accepted 11 April 2021
Accepted manuscript posted online 21 April 2021
Published 10 June 2021

The HIV-1 envelope glycoprotein (Env) is a virion surface protein that mediates viral entry into target cells. Proper Env functioning in the entry step is a prerequisite for efficient virus replication (1–4). The HIV-1 Env precursor protein gp160 is cotranslationally glycosylated in the endoplasmic reticulum, transported to the Golgi, and cleaved by a cellular protease to yield gp120 and gp41 proteins. The Env-spike structure protruding from the virion surface is formed by a trimer composed of the gp120-gp41 heterodimer. In the virus entry stage, gp120 binds to cellular receptor CD4 and coreceptor CCR5/CXCR4, and gp41 is involved in the subsequent fusion process. Since HIV-1 virions usually contain a small number (~14) of Env spikes (5, 6), the interaction of Env-gp120 and receptor/coreceptor molecules for virus entry is very likely to be efficient.

Based on sequence variations, gp120 is divided into conserved (C1 to C5) and variable (V1 to V5) domains (Fig. 1) (1–4). Structural analyses of HIV-1 Env trimer in a prefusion state revealed that the close association of V1/V2 and V3 loops forms the apex of the trimer and contributes to the stability of the Env trimer structure (Fig. 2A) (7, 8). Meanwhile, it is well recognized that HIV-1 Env is highly mutable and adaptable to various environments, and that mutations in gp120, including the V1/V2 and V3 loops, strongly affect virus phenotypes such as viral fusogenic activity, viral infectivity, and neutralization sensitivity (9–13). The initial steps for HIV-1 entry into the target cells have long been believed to be as follows. Upon binding to CD4, Env-gp120 changes conformation to allow the V3 loop to interact with CCR5, and this association sequentially activates conformational changes of Env-gp41 to trigger virus-cell fusion (2–4, 14). Several lines of evidence showed the molecular intercourse of CCR5 and HIV-1 Env-gp120. The extracellular N-terminal segment of CCR5 interacts with the V3 loop stem and Env-gp120 bridging sheet, which is exposed only after CD4 binding, whereas the V3 loop tip binds to the CCR5 chemokine recognition site 2 (CRS2) pocket, including extracellular loop 2 (ECL2) (Fig. 2B) (15–19). However, a recent analysis of the CD4-full-length gp120-unliganded CCR5 complex by cryo-electron microscopy (cryo-EM) provided a quite different picture of HIV-1 entry (20). Structural comparison of the CD4-gp120-CCR5 and CD4-gp120 complexes demonstrated no obvious conformational changes of gp120, suggesting that the binding of gp120 to CCR5 does not induce the conformational change of gp41 (20). The authors proposed that the role of CCR5 as a coreceptor for HIV-1 is to stabilize CD4-induced conformation of Env-gp120 and to bring Env-gp41 into close proximity to the plasma membrane (20). Since HIV-1 Env sequences and their phenotypes are highly variable, it is important to perform functional studies on various gp120s carrying a distinct V3 loop in order to elucidate their CD4- and CCR5-interacting activity.

The fundamental and most evident property of viruses is their high ability to evolve themselves under various environments. To better understand viral mutations and adaptation, we have been studying how HIV-1 acquires an improved replication capacity in growth-restricted conditions using macaque-tropic HIV-1s (HIV-1mts) as model viruses. We and others have experimentally identified various adaptive mutations within Env-gp120 using macaque cells and macaque individuals infected with HIV-1mt derivatives, or chimeric viruses between SIV and HIV-1 (SHIVs) (21–27). In our adaptation experiments using a CCR5-tropic HIV-1mt (NL-DT562, abbreviated as 562) and a cynomolgus macaque (CyM) lymphocyte cell line, we found spontaneous mutations located at the V1/V2 and V3 loops in Env-gp120, and confirmed their enhancing effects on the viral growth potential in the CyM cell line (Fig. 1) (26, 27). While V3 loop sequences are highly variable among different strains of HIV-1, it is well known that in a motif at the V3 loop tip, 312GPGR(Q)315 (by HXB2 numbering), there exist highly conserved GPG triplet residues (Fig. 1) (28, 29). Mutations in the GPGR motif have been reported to exhibit deleterious effects on HIV-1 replication in human cells (9, 11). In contrast, an adaptive mutation (G312V) in the GPGR motif, which was found in SHIV from a prolonged, infected culture of pig-tailed macaque (ptm) lymphocytes, enhances viral infectivity by increasing the ptm CD4-mediated entry (21, 24, 25). In this study, we show that an adaptive mutation, G310R, which we identified in the conserved motif at the V3 tip (308GPGR311 by 562 numbering) (Fig. 1 and 2), drastically affects viral

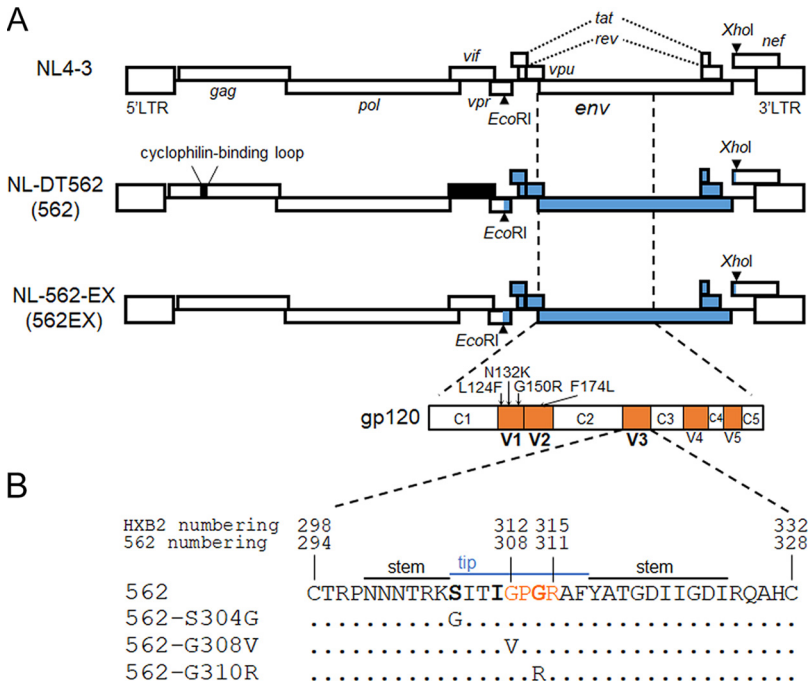

FIG 1 Genome organization and Env-gp120 glycoprotein. (A) Genome structures of HIV-1 clones used in this study and the domain structure of gp120. Genome organization of authentic HIV-1 (NL4-3) (49), prototype CCR5-tropic HIV-1mt (NL-DT562) (26), and newly constructed HIV-1 (NL-562-EX) clones are presented. Black and blue boxes indicate regions derived from SIVmac (SIVmac239) (61), and HIV-1 (SF162) (62), respectively. The enlarged gp120 region is presented. Constant (C1 to C5) and variable (V1 to V5) domains in gp120 are shown by white and orange areas, respectively. Four adaptive mutations in the V1/V2 loop of gp120 that we previously identified (27) are indicated. (B) Amino acid sequences of the V3 loops. Amino acid sequences of the V3 loops from parental 562 and its mutants carrying a single-amino-acid adaptive mutation are aligned. Numbers indicate amino acid positions in the Env proteins of HXB2 (GenBank M38432) and 562 (26) as shown. Bold letters in the 562 line show the residues for which we identified an adaptive mutation (27). The V3 tip and stem regions are indicated by blue and black lines/letters, respectively. Orange letters show the GPGR motif. The alignment was performed by Genetyx ver.14.

replication in a species-specific manner. We aimed to gain molecular details as to how the adaptive mutations at the V3 tip (G308V and G310R by 562 numbering) affect the interactions of Env-gp120 with CD4 and CCR5. The obtained data illustrate a previously unrecognized regulation mechanism of Env-receptor interactions by the V3 tip.

RESULTS

G310R mutation in the GPGR motif at the V3 tip of 562 promotes viral growth in macaque cells but abolishes infectivity in human cells. Taking advantage of the high ability of HIV-1mts to adapt in restrictive environments imposed by macaque cells, we have studied the viral mutation and adaptation process (23, 26, 27, 30, 31). A CCR5-tropic HIV-1mt clone 562 carrying the *env* gene of an HIV-1 subtype B SF162 clone was generated by genetically modifying a portion of the *gag* gene encoding the cyclophilin-binding loop and the entire *vif* gene (Fig. 1A) (26, 27). By adaptation of 562 in CyM cells (26, 30), while a number of mutations throughout the genome were noted, adaptive mutations that highly enhance the viral replication ability were identified within the V1/V2 loop (L124F, N132K, G150R, and F174L) and V3 loop (S304G, I307V, and G310R) of Env-gp120 (Fig. 1B) (26, 27).

To confirm the above adaptive mutations that emerged in macaque cell cultures promote viral replication both in macaque and human cells, we monitored the growth properties of parental 562 and its Env mutant clones in HSC-F (CyM) and MT4/R5 (human) lymphocyte cell lines. Viruses were prepared from 293T cells transfected with proviral clones, and equal amounts of viruses were inoculated into each cell line. Consistent with our previous results (27), all adaptive mutations enhanced the viral growth ability in

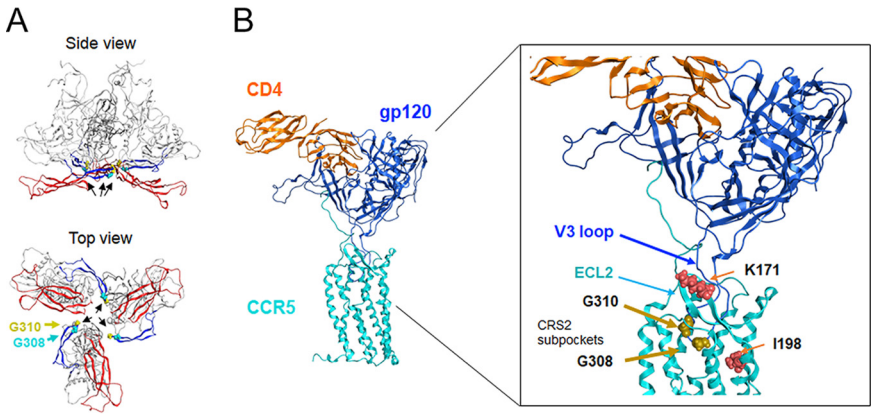

FIG 2 Structure of HIV-1 Env-gp120. (A) Overall architecture of a full-length HIV-1 Env gp120 trimer model in the unliganded state (27). The V1/V2 and V3 loops are highlighted in red and blue, respectively. Arrows indicate the locations of the V3 loop tips in the gp120 trimer. The locations of the V3 tip residues that were analyzed in the present study are shown by yellow and blue spheres. (B) Overall (left) and enlarged (right) views of a full-length HIV-1 Env gp120 monomer model in the CD4 and CCR5 bound state. The model was constructed by homology modeling using the cryo-EM structure of the HIV-1 CD4-gp120-CCR5 ternary complex (PDB code 6MEO) (20), followed by MD simulation for 100 ns (see the Materials and Methods for details). In the enlarged view, brown and poppy red spheres indicate amino acid residues at the V3 tip (G308 and G310) and those in CCR5 (K171 and I198), respectively. G308 and G310 residues are present in the conserved GPG triplet residues at the V3 tip. K171 and I198 residues are located at the ECL2 and TM5 domains in CCR5, respectively. These residues differ between human and CyM CCR5s.

HSC-F cells (Fig. 3A). In sharp contrast, G310R did not grow at all in MT4/R5 cells, while all the other mutants grew better than the parental 562 virus (Fig. 3B). To further ascertain the replication-defect of G310R in human cells, we tested 562 and G310R for viral infectivity in TZM-bl cells, HeLa-derived cells stably expressing human CD4/CCR5/CXCR4. Notably, the infectivity of G310R was almost negligible in the TZM-bl cells (Fig. 3C). These results indicate that the adaptive mutations examined, except for G310R, significantly increase the viral growth potential in both macaque and human cells. Unexpectedly, G310R conferred a unique biological phenotype, i.e., a species-specific growth ability, on HIV-1mt clone 562.

The charged property of amino acids at positions 308 and 310 of Env-gp120 may be associated with the species-specific viral growth of 562. We previously reported the frequency of amino acid residues at position 310 (by 562 numbering) of Env sequences in an HIV-1 subtype B population (27). While authentic G310 is highly conserved (around 98%), adaptive 310R is also found in the population (around 0.2%) (Fig. 4A). To examine the effect of the amino acid property at position 310 on 562 growth, we chose L (higher frequency than R), E (negative charged residue, opposite to R), and K (positive charged residue, same as R), and newly constructed proviral clones designated G310L, G310E, and G310K (Fig. 4A) for multicycle replication assays. On one hand, an adaptive mutation G312V (by HXB2 numbering) was found in an adaptation experiment using ptm lymphocytes infected with a SHIV carrying the *env* gene from a subtype A HIV-1 strain (21, 24, 25). Virological analysis showed that SHIV with the G312V mutation, but not the parental virus, exhibited enhanced infectivity due to the increased ptmCD4-mediated entry process (21, 24, 25). It has also been reported that when G312V was introduced into *env* genes of seven different HIV-1 isolates, five Env proteins were found to be effective for augmented viral entry into target cells via human and macaque CD4, whereas the other two did not utilize human CD4 or macaque CD4 (21, 24, 25). At the same position as G312 (G308 by 562 numbering), we previously identified an adaptive G308E mutation in 562 (27). Since G308 and G310 are located at the GPGR motif within the V3 tip (Fig. 1 and 2), we also compared the effects of amino acids replaced at these positions on viral growth in macaque and human cells (Fig. 4B). As observed in Fig. 3, proviral clone 562 grew relatively poorly in human MT4/R5 cells. This may be due to the lack of a cyclophilin-binding loop in 562

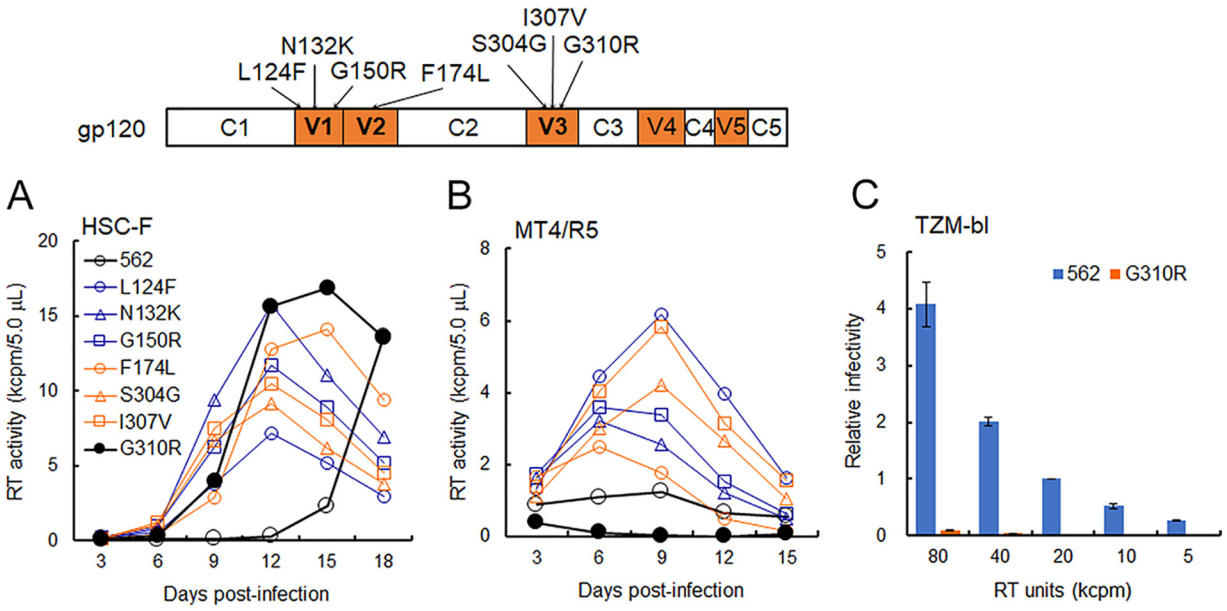

FIG 3 Replication properties of parental 562 and its Env variant clones carrying an adaptive mutation. (A and B) Growth kinetics in lymphocyte cells. The schematic of Env-gp120 organization from Fig. 1 is presented at the top for clarity. Viruses prepared from 293T cells transfected with the indicated proviral clones were inoculated into CyM HSC-F (A) and human MT4/R5 (B) cells, and virus replication was monitored by the virion-associated RT activity in the culture supernatants. Equal amounts of viruses (2×10^6 RT units) were used for inoculation into HSC-F cells (2×10^5 cells). For the spin-infection of MT4/R5 cells (1×10^5 cells), equal amounts of viruses (6×10^6 RT units) were used. Representative data from three independent experiments are shown. Sample symbols in panel (B) are the same as those in panel (A). (C) Infectivity of 562 and G310R in TZM-bl cells. Viruses were inoculated into TZM-bl cells as described in the Materials and Methods, and 2 days postinfection, cells were lysed for luciferase assays. Viral infectivity relative to that for 562 in cells inoculated with 20 RT units (kcpm) was calculated by relative light units in cell lysates. Mean values ± standard errors (SEs) are shown ($n = 3$).

capsid, leading to the increase in the inhibitory effect of human TRIM5alpha and/or to the decrease in interactions with factors (e.g., cyclophilin A and Nup358) necessary for nuclear entry of the HIV-1 genome (Fig. 1A) (32, 33). To avoid this issue, we generated a series of new proviral clones, NL-562-EX (562EX) and its Env mutant clones, which have *gag* and *vif* genes from an authentic HIV-1 clone, NL4-3 (Fig. 1A). Thus, for CyM HSC-F and human MT4/R5 infections after this point in the study, 562 (and its derivative) and 562EX (and its derivative) clones were used, respectively. Of the Env V3 tip mutants (S304G, G308V/E, and G310R/L/E/K), S304G was used as a positive control for enhanced growth potential in both CyM and human cells. As shown in Fig. 4B, the positive-control S304G mutants displayed a higher replication ability relative to the parental clones in CyM and human cells. In CyM cells, all mutants tested grew better, to various degrees, than the parental clone 562. For example, the G310L mutant showed a similar growth ability to that of the S304G mutant, whereas G308E grew slightly better than 562, as we previously reported (27). Intriguingly, in human cells, while G308V and G310L grew better than the parental 562EX to a similar extent with S304G (note the peak days for virus production), the other clones (G308E, G310E, G310K, and G310R) exhibited extremely low or undetectable viral growth. These results may imply that the charged amino acids at positions 308 and 310 of 562 Env are responsible for the observed species-specific growth phenotype. Taken together, our results here suggest that the property of the amino acid replaced within the conserved motif at the V3 tip exerts distinct effects on the virus growth potential of a 562 proviral clone.

Molecular dynamics simulations suggest that G310R, but not G308V, severely impedes the human CD4-gp120 interaction. To assess the effects of the adaptive mutations (G308V and G310R) within the V3 tip on molecular interactions of gp120 and receptors, we performed a molecular dynamics (MD)-based *in silico* mutagenesis study as described previously (27, 34–36) (Fig. 5). We constructed various ternary complex models consisting of distinct combinations of the three components of the complex, 562 Env-gp120, CD4, and CCR5. The complex models were subjected to MD

A

Amino acid	Number	Frequency (%)
Aliphatic		
G	19101	98.002
L	222	1.138
A	7	0.036
M	6	0.031
Basic		
R	47	0.242
K	1	0.005
Acidic		
E	40	0.206
Neutral hydrophilic		
S	11	0.057
Aromatic		
W	36	0.185
F	1	0.005
(-) or X	19	0.001

B

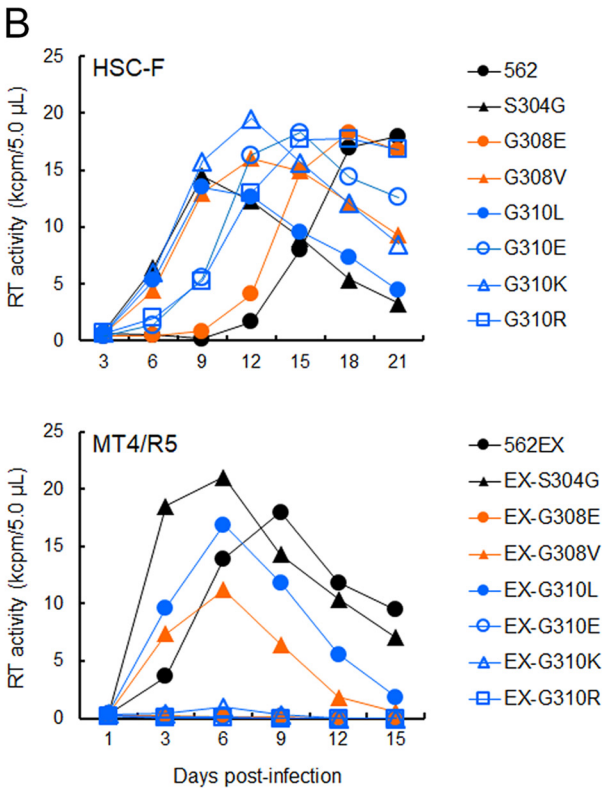

FIG 4 Effect of mutations in the V3 tip region on virus replication. (A) Frequency of amino acids at position 310 of Env-gp120 (by 562 numbering). Authentic (blue), adaptive (green), and selected (orange) amino acids are shown. Env sequences in the HIV-1 subtype B population ($n = 19{,}419$) were obtained from the HIV Sequence Database (http://www.hiv.lanl.gov/content/sequence/HIV/mainpage.html) (27). (B) Infection experiments of 562, 562EX, and their V3 mutants. The *env* sequences of 562 and 562EX are identical, and Env mutant clones (S304G, G308V/E, and G310R/L/E/K) in the context of 562 and 562 EX were constructed. Viruses prepared from 293T cells transfected with the indicated proviral clones were inoculated into HSC-F (upper) and MT4/R5 (lower) cells, and virus replication was monitored by the virion-associated RT activity in the culture supernatants. HSC-F cells (2×10^5 cells) and MT4/R5 cells (1×10^5 cells) were infected with equal amounts of viruses (5×10^5 RT units for HSC-F and 2×10^5 RT units for MT4/R5). Infection of MT4/R5 cells was performed by the spin-infection method. Representative data from three independent experiments are shown.

simulations to characterize structural dynamics in solution. Figure 5A shows the complex structures at 100 ns of MD simulations. There were variations in the orientation of the gp120/CD4 complex with respect to CCR5 embedded in the lipid bilayer. The most prominent change in the orientation was seen with the G310R gp120 bond to human receptors (Fig. 5A, upper middle panel). The results suggest that the ternary complex had variable rotational flexibility on the plasma membrane.

The structural changes of the receptor-binding surfaces of 562 Env-gp120 during the MD simulations were monitored by root mean square deviations (RMSDs) (Fig. 5B and C) (27, 34–36). The RMSDs remained almost unchanged with the gp120-binding surfaces for CD4 and CCR5 in all the complexes studied, suggesting that the receptor-binding surfaces largely maintained their initial structures during the simulations. We then analyzed the root mean square fluctuation (RMSF) to assess the structural fluctuation of the individual amino acids of the gp120 binding surfaces (27, 34–36). The RMSFs were within the levels of background fluctuations of gp120 in solution (Fig. 5D and E). This was in sharp contrast to the previous observations with the ligand-free gp120, where the loop regions involved in receptor binding, such as the V3 loop, heavily fluctuated (27, 34–36). Collectively, the RMSD and RMSF data strongly suggest that the structural dynamics of the gp120 binding surfaces were markedly suppressed in the ternary complexes, being at a state of thermodynamic equilibrium during the present MD simulations.

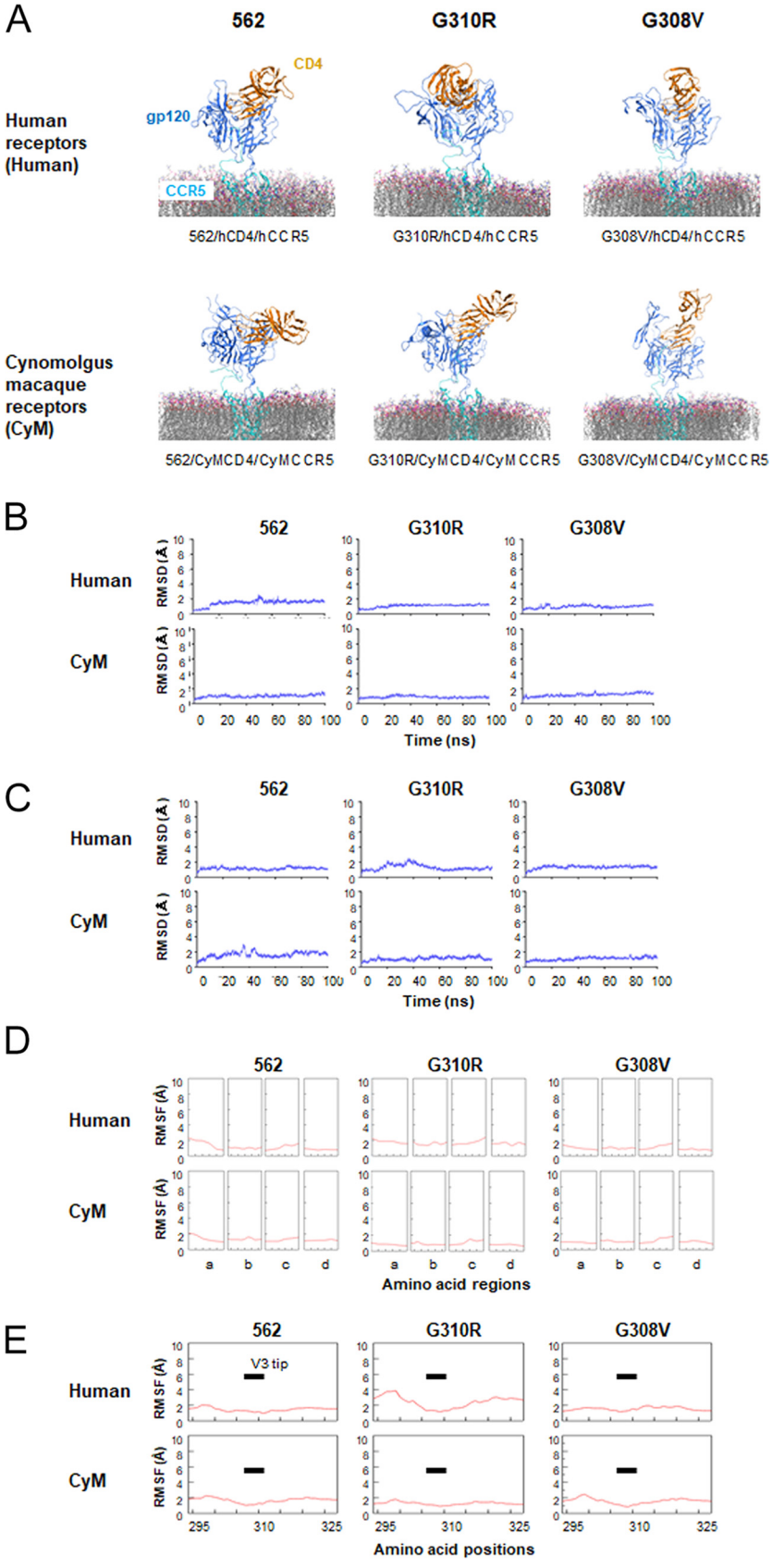

FIG 5 MD simulations of CD4-562 Env-gp120-CCR5 ternary complexes embedded in a lipid bilayer. (A) The CD4-gp120-CCR5 complex models were constructed by homology modeling and MD simulations

(Continued on next page)

On the basis of these data, we estimated the binding free energies of 562 Env-gp120 to CD4 and CCR5 using independent all atom MD trajectories ($n = 100$) from 95 to 100 ns of MD simulations (Fig. 6A). The parental 562 virus, whose growth was poor in CyM cells (Fig. 3 and 4), was estimated to have a very weak affinity to CyM CD4 (Fig. 6A, 562). Impressively, the G310R substitution selectively abolished the binding ability of gp120 to human CD4 alone (Fig. 6A, G310R). The results were consistent with the negligible growth ability of G310R in human cells (Fig. 3 and 4). Such a selective defect in the gp120 binding ability was not detected with the G308V mutant (Fig. 6A, G308V). These results suggest that the G310R substitution at a site away from the CD4 interaction site (Fig. 2B) may strongly diminish the binding ability of gp120 to human CD4 in the 562 Env backbone.

Structural changes associated with the selective defect of the G310R mutant were evaluated by the superpositions of the complex structures during the MD simulations (Fig. 6B). A distinguishing change was detected around the gp120-CD4 interface. The bridging sheet, which is composed of four antiparallel β-sheets in the C4 and V1/V2 base regions (27, 37), was placed most distantly from the apex of the CD4 molecule in the G310R gp120 bond to human receptors (Fig. 6B, upper middle panel). In association with this, the orientation of CD4 on gp120 was distinguishable from the others in the G310R gp120 bond to human receptors (Fig. 6C, upper middle panel). In contrast, G310R substitution did not induce apparent repositioning of the bridging sheet and CD4 on gp120 in the ternary complex of CyM CD4-gp120-CyM CCR5 (Fig. 6B and C, lower panels). These results suggest that the G310R substitution in 562 Env influences most prominently, among the complexes tested, the binding mode of gp120 to human CD4.

G310R mutation in 562 Env-gp120 reduces the capacity of the virus to bind to human cells, but not to macaque cells. Our *in silico* structural analysis predicted that the G308V and G310R mutations within 562 Env V3 tip can affect the viral binding ability to CD4 and CCR5 (Fig. 6). In addition, since G308V was found in the SHIV adaptation experiment as a mutation that increases the ptmCD4-mediated virus entry (21, 24, 25), we asked if the G310R mutation also affects viral ability to bind to CyM and human cells via CD4. First, we determined the expression levels of CD4 on CyM HSC-F and human MT4/R5 cell surfaces by flow cytometry (FACS) analysis. As shown in Fig. 7A, the expression level of CD4 on the HSC-F cell surface was slightly higher than that on the MT4/R5 surface. Next, we performed virus-binding assays as reported previously (27). Viruses were prepared from 293T cells transfected with 562EX or 562EX-G310R. Virus samples were inoculated into HSC-F and MT4/R5 cells, incubated at 4°C for 2 h, and cell lysates were prepared for the assays. The p24 amounts in the cell lysates were determined for indices of virus-cell binding. Heat-inactivated samples for each virus were used as negative controls. In HSC-F cells, no significant difference in the viral binding ability between 562EX and 562EX-G310R was observed (Fig. 7B). On the other hand, in MT4/R5 cells, the binding ability of 562EX-G310R was impaired relative to that of 562EX (approximately by half) (Fig. 7B). While these data were not as marked as expected from those obtained by *in silico* analyses, the above results as a whole (Fig. 6 and 7) demonstrate that the G310R mutation reduces the viral binding

FIG 5 Legend (Continued)
at 1 bar and at 310 K for 100 ns in 0.15 M NaCl. Complex structures at 100 ns of MD simulations are shown. Individual complexes are viewed from the same direction by aligning along human CCR5s in the lipid bilayer. (B and C) The RMSDs of the receptor binding surfaces during 0 to 100 ns of MD simulations were calculated using the cpptraj module in AmberTools 16 as described previously (27, 36). (B) RMSDs of the gp120 regions for CD4 binding (37) during the MD simulations. The binding regions are composed of amino acid residues T246 to T251, Q359 to M369 (CD4 binding loop), T445 to E421, and R460 to D465 in 562 gp120. (C) RMSDs of the V3 loop (C294 to C328) of the 562 gp120 regions for CCR5 binding (20). (D and E) The RMSFs of the receptor binding surfaces during 90 to 100 ns of MD simulations were calculated using the ptraj module (60) in AmberTools 16 (27, 34–36). (D) RMSFs of the gp120 regions for CD4 binding (37). The regions indicated as a, b, c, and d are T246 to T251, Q359 to M369, T445 to E421, and R460 to D465 in 562 gp120 (26, 27), respectively. (E) RMSFs of the V3 loop (C294 to C328) of the 562 gp120 regions for CCR5 binding (20).

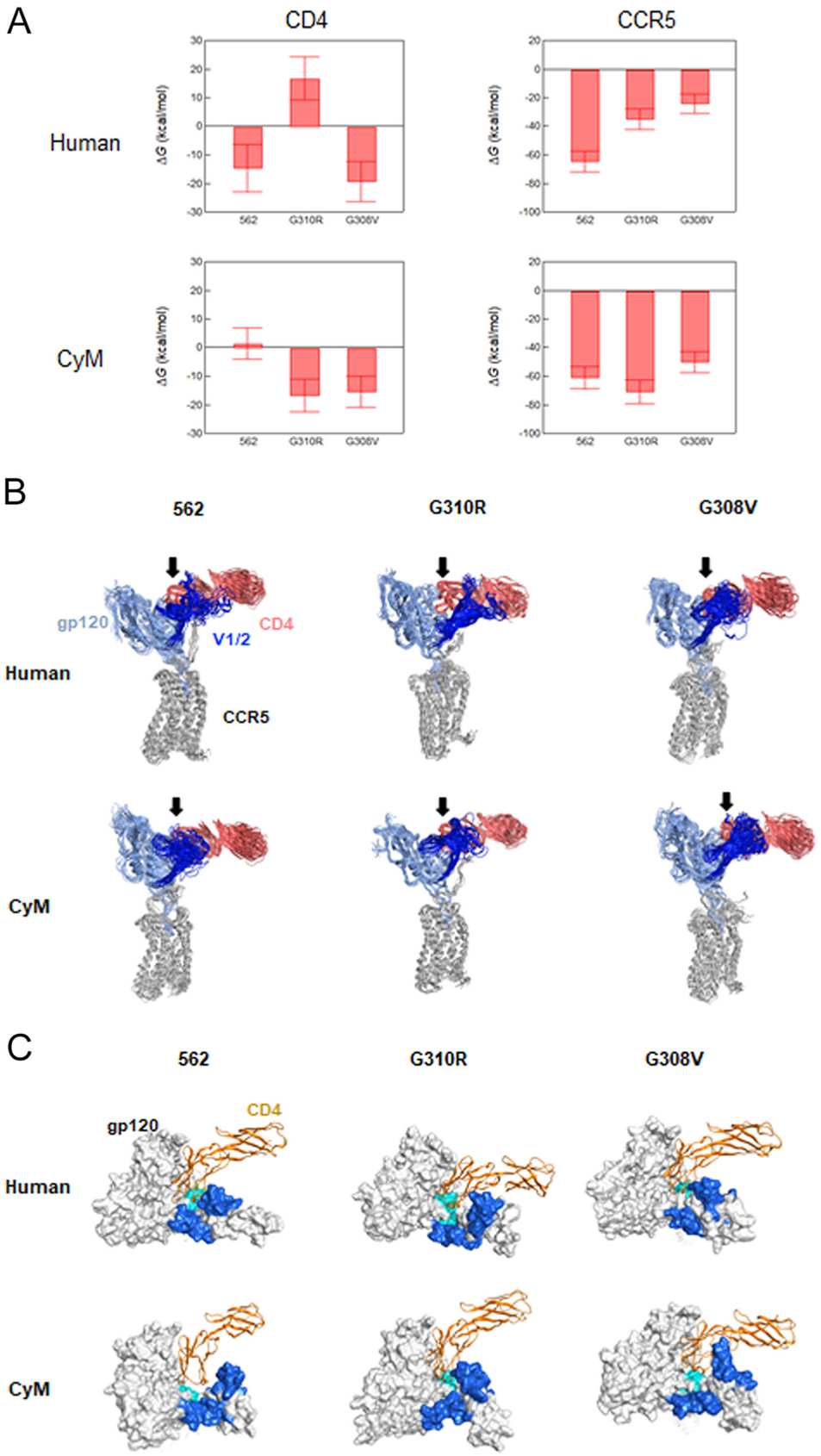

FIG 6 Effects of single-amino acid substitutions at the 562 Env-gp120 V3 tip on interactions of gp120 with CD4 and CCR5. (A) Binding free energies. The CD4-gp120-CCR5 ternary complex models from independent all-atom MD trajectories of the last 5 ns after 100 ns of MD simulations were used to

(Continued on next page)

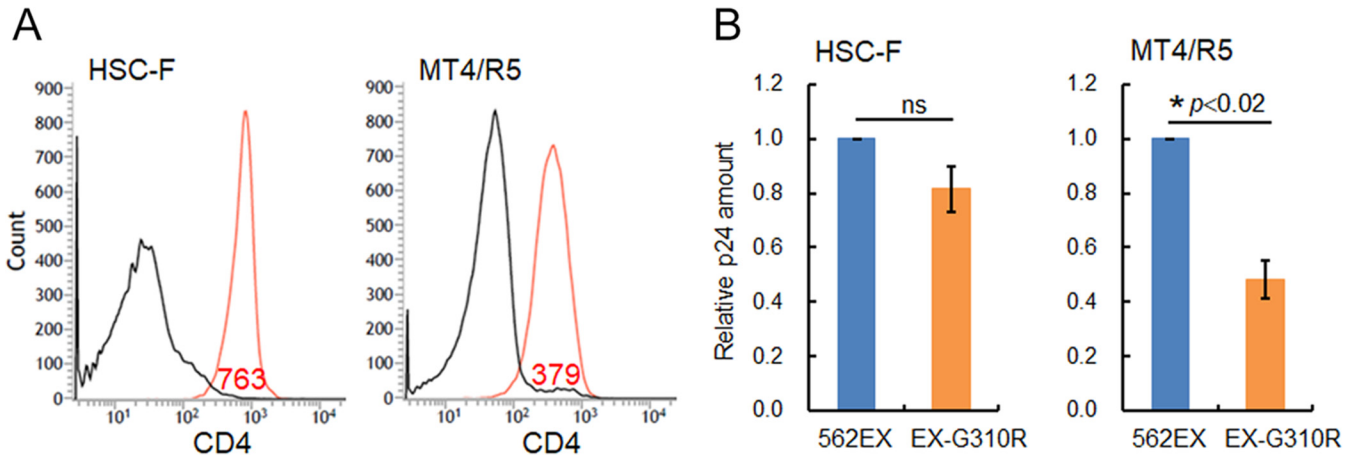

FIG 7 Effect of the G310R mutation on the viral ability to bind to CyM HSC-F and human MT4/R5 cells. (A) CD4 expression levels on the HSC-F and MT4/R5 cell surfaces. Cells were stained with FITC-labeled CD4 antibody and analyzed by a flow cytometer. Numbers in the graphs indicate the mean fluorescence intensity of cell surface CD4. Negative controls are shown by black lines. (B) Viral ability to bind to HSC-F and MT4/R5 cells. Virus binding assays were performed as described in the Materials and Methods. Relative virus binding ability (Gag-p24 for EX-G310R/Gag-p24 for 562EX) is presented. Mean values ± SEs from three independent experiments are shown. Significance relative to control 562EX was determined by the Welch's *t* test; ns, not significant.

ability to human cells but does not significantly affect viral binding to CyM cells. The outward difference may come from the two measurement systems used, i.e., assays for the interaction of trimeric and monomeric gp120 in experimental and *in silico* systems, respectively. In conclusion, our results here show that the G310R mutation species-specifically affects the binding capacity of 562 to host cells.

The replication defect of the G310R mutant in human cells is relieved by a single-amino acid replacement from human CCR5 to CyM CCR5 at position 198. It is well established that the V3 loop in gp120 plays a critical role in the HIV-1 Env-CCR5 interaction (1–4). Thus, we sought to identify a determinant(s) in CCR5 responsible for the defective phenotype of the V3 tip mutant G310R in human cells. Amino acid sequences of CyM and human CCR5 are well conserved (97% identity) and differ only by eight amino acids, located at the extracellular N-terminal segment (N-term), transmembrane helix (TM) 1, TM2, TM3, ECL2, and TM5. It has been reported that anti-human CCR5 antibodies, designated clones 3A9 and 2D7, are specific for the N-term and ECL2 of CCR5, respectively (38). We found that it is difficult to recognize CyM CCR5 using 2D7, suggesting some difference in the region around ECL2 between CyM and human (our unpublished data). Extensive structural and functional analyses on the CCR5 and gp120 interaction has revealed that the conformation of ECL2 modulates the overall structure of CCR5, thereby changing the interaction mode between the two molecules (39). The ECL2 of CCR5 has been also shown to contact the residues at the tip and stem of the V3 loop by structural analysis (20) (Fig. 2B). Therefore, we paid attention to the different amino acid residues at positions 171 and 198 around the ECL2 region of CyM and human CCR5 proteins (Fig. 8A). First, we constructed various plasmid vectors that express CyM CCR5, human CCR5, and its mutants possessing one of the amino acid substitutions K171R, I198M, or both (K171R/I198M) for virus infectivity assays. These expression vectors were then transfected into MAGI cells, which are positive for human CD4 and CXCR4 but negative for CCR5. Transient expression levels of surface CCR5 on the transfected cells were monitored by FACS analysis and confirmed to be similar among

FIG 6 Legend (Continued)
calculate the binding free energies of the indicated receptor molecules using MMPBSA.py (59) in AmberTools16 (AMBER 2016, University of California, San Francisco). Mean values ± SEs are shown ($n = 100$). (B) Overall views of the ternary complex structures. The structures during 50 to 100 ns of MD simulations ($n = 10$) were superposed with CCR5, and the side views are shown. Arrows indicate the CD4 apex region for gp120 binding. (C) Top views of the ternary complexes at 100 ns of MD simulations. Location of the gp120 bridging sheets (37) and the V1/V2 region are indicated by cyan and blue, respectively.

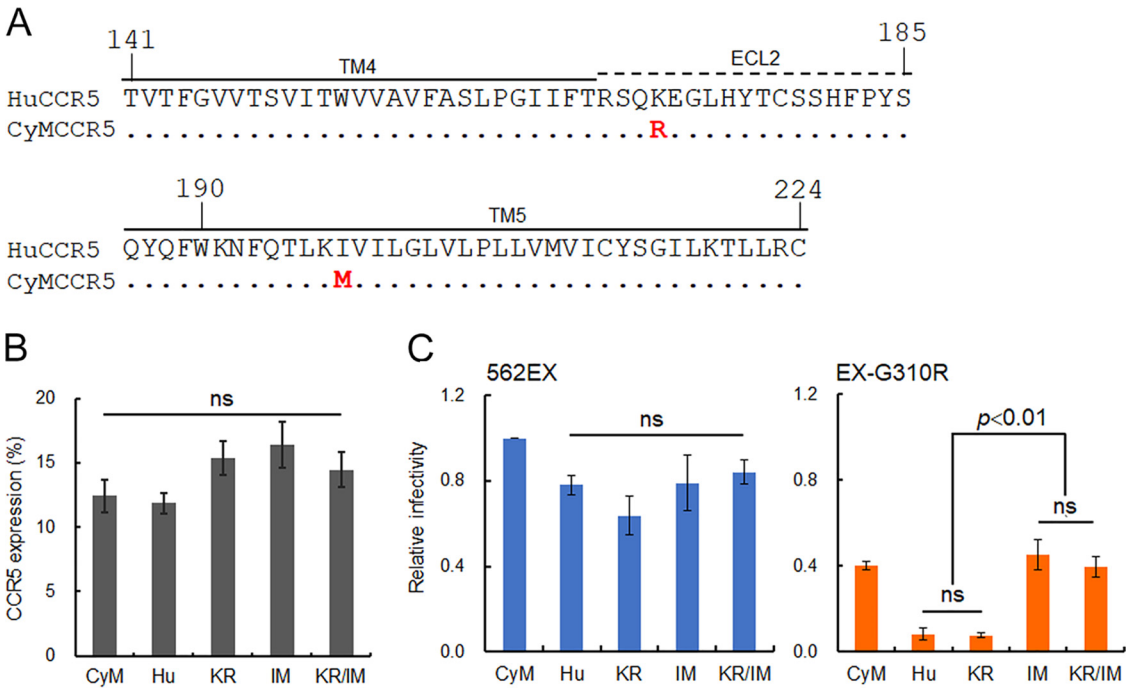

FIG 8 Effect of various CCR5 expression levels on the infectivity of 562EX and 562EX-G310R (EX-G310R). (A) Alignment of human and CyM CCR5 amino acid sequences. Amino acid sequences from TM4 to TM5 in CCR5 (based on GPCRdb ccr5_human, https://gpcrdb.org/) are shown. TM4, ECL2, and TM5 regions are as indicated. Red letters show the different residues between CyM and human CCR5s. Alignment was performed by Genetyx ver.14. (B) The CCR5 expression level on the cell surface. MAGI cells were transfected with the indicated CCR5 expression vectors and, at 24 h posttransfection, cells were stained with anti-human CCR5 antibody for FACS analysis. Mean values ± SEs ($n = 6$) are shown. Significance was evaluated by the likelihood-ratio chi-squared test ($n = 6$); ns, not significant. (C) Infectivity of 562EX and 562EX-G310R in various CCR5-expressing cells. Viruses were prepared from 293T cells transfected with the proviral clones, and equal amounts of viruses were inoculated into MAGI cells transiently expressing various CCR5s. On day 2 postinfection, cells were lysed for beta-galactosidase assays. Viral infectivity relative to that for 562EX in CyM CCR5-expressing cells is shown. Mean values ± SEs ($n = 5$) are shown. Significance was determined by the Welch's *t* test ($n = 5$); ns, not significant. Hu, human; KR, K171R; IM, I198M; KR/IM, K171R/I198M.

transfected MAGI cells (Fig. 8B). Next, virus samples prepared from 293T cells transfected with the proviral clones (562EX or 562EX-G310R) were inoculated into the transfected MAGI cells. As shown in Fig. 8C (left panel), while 562EX infectivity in human CCR5-expressing cells was lower than that in CyM CCR5-expressing cells, it was quite similar among cells expressing human CCR5 or its mutants (K171R, I198M, and K171R/I198M). This was probably attributable to amino acid differences in human and CyM CCR5 proteins other than the targeted area and did not affect interpreting the results obtained. In sharp contrast, 562EX-G310R infectivity varied greatly among cells expressing human CCR5 or its mutants (Fig. 8C, right panel). In agreement with the viral binding ability to human cells (Fig. 7), 562EX-G310R infectivity in MAGI cells expressing CyM CCR5 was reduced to approximately 40% relative to that of 562EX. This reduction in infectivity implicates the decreased binding ability of 562EX-G310R to human CD4. Moreover, 562EX-G310R displayed an approximately 5-fold reduction in infectivity to MAGI cells expressing human CCR5 compared to the cells expressing CyM CCR5, suggesting inefficient binding to human CCR5. In human CCR5 K171R-expressing cells, 562EX-G310R also exhibited decreased infectivity similar to that in human CCR5-expressing cells. Importantly, in cells expressing human CCR5 I198M, the infectivity of 562EX-G310R was recovered to a comparable level to that in CyM CCR5-expressing cells. This enhanced infectivity was also observed in human CCR5 K171R/I198M-expressing cells (Fig. 8C, right panel). These results demonstrate that the isoleucine residue at position 198 in TM5 of human CCR5 is principally responsible for the CCR5-mediated reduction of 562EX-G310R infectivity in human cells.

DISCUSSION

In this study, we aimed to elucidate molecular bases underlying the regulation of HIV-1 infection and adaptation by characterizing the biological and structural impacts of a unique amino acid substitution, G310R, at the V3 loop tip in 562 Env-gp120 (Fig. 1, 2, and 5). Virological analyses showed that a G310R substitution in 562 Env-gp120 selectively abolished the viral replication ability in human cells despite evoking the augmentation of viral replication in CyM cells (Fig. 3). Interestingly, our mutational analyses suggested that the observed species-specific effects can be attributed to the charged property of amino acid residues at positions 308 and 310 of 562 Env-gp120 (Fig. 4). The results are consistent with the data on the G310R changes in the 562 Env-gp120 binding ability to CD4 (Fig. 6) and with cell-based viral binding assays (Fig. 7). Furthermore, we confirmed the species-specific effects of the G310R substitution on the gp120-CCR5 interaction by MD simulations (Fig. 6) and virus infection experiments using various CCR5-expressing cells (Fig. 8). Collectively, our data indicate that residue 310 at the V3 loop tip is a key regulator for forming a stable CD4-gp120-CCR5 complex for viral infectivity and adaptability. This conclusion agrees with our previous observation that suggests a unique structural change in G310R gp120 for reducing the viral sensitivity to a CCR5 antagonist (27). A recent cryo-EM analysis suggested that CCR5 functions to stabilize CD4-induced gp120 structure and to bring Env-gp41 into proximity to the plasma membrane (20). Thus, mutations of amino acid residues that participate in the binding with CD4 and/or CCR5 may potentially influence the interactions of Env-gp120 with both CD4 and CCR5. Our results in this study, that the G310R mutation in 562 Env-gp120 exerts the species-specific effect by affecting interactions of Env-gp120 with both CD4 and CCR5 molecules, are in line with this prediction. Further studies are required to phenotypically and mechanistically determine the mutational effects of Env-gp120 on its interactions with CD4 and/or CCR5.

The G310R substitution in 562 Env strongly affected the CD4 binding ability in a species-specific manner (Fig. 6 and 7) despite it occurring at a site away from the CD4-binding region of gp120 (Fig. 2B). The results indicate *cis*-allosteric effects of the G310R substitution on the CD4-binding surfaces of HIV-1 gp120. Previous site-directed mutagenesis studies, along with the structural study of gp120 lacking most of the V1/V2 loop region, showed that the CD4-binding surfaces are formed with discontinuous gp120 segments (37, 40–42). Notably, our present MD simulations predict that the G310R substitution selectively induces relocation of the bridging sheet away from the side of the CD4 apex (Fig. 6B, upper middle panel). These results suggest that the 3-D position of the bridging sheet plays a key role in the stability of the gp120-CD4 complex. This conclusion is consistent with the results of gp120 mutagenesis in this region (23, 40, 42) and the MD simulation of the full-length gp120-CD4 binary complex (20, 27, 43).

Importantly, the present study provides new insights into the regulation of the gp120-CD4 interaction. Unlike previous structural studies, full-length gp120s with a complete V1/V2 loop were analyzed in this work. Consequently, we could evaluate for the first time the molecular interactions that connect distinct regions of gp120 that have the V1/V2 region (Fig. 9A). Notably, the hydrogen bond between the R416 residue at the β20-β21 loop in the gp120 bridging sheet (37) and S67 residue at the apex of CD4 was formed in the 562 gp120 complex, whereas it was lost in the G310R gp120 complex, along with translocation of the V1/V2 loop (Fig. 9A). The hydrogen bond between the R324 residue in the V3 base and Q412 in the bridging sheet was formed in both gp120 complexes. These results suggest the presence of intra- and intermolecule interactions that connect V3, the bridging sheet, and the apex of CD4. In addition, the conformational change of the R416 residue at the contact site with CD4 may be involved in the alteration in the CD4 binding mode.

Present mutagenesis study demonstrates that the species-specific phenotype of the 562 clone is dependent on the charged state of amino acid residues at positions 308 and 310 in the V3 region (Fig. 4). The finding is consistent with our previous report that

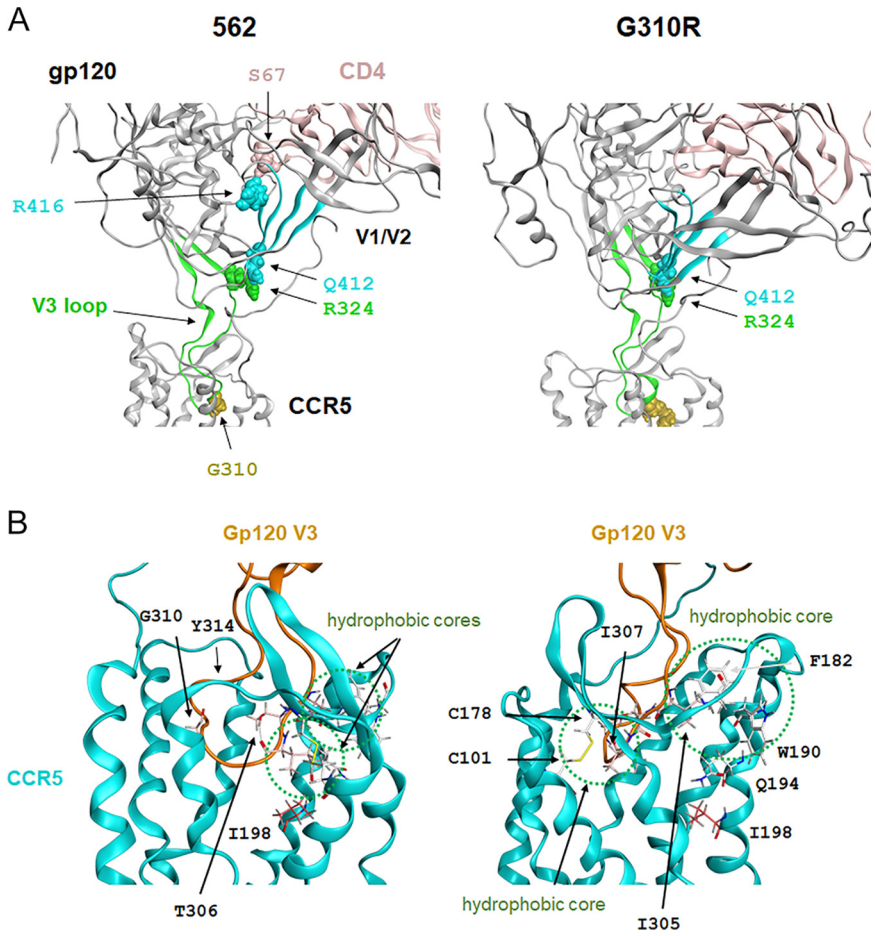

FIG 9 Molecular interactions among CD4, 562 Env-gp120, and CCR5. (A) Enlarged views of the human CD4-gp120 interaction site in the ternary complexes at 100 ns of MD simulation. Spheres indicate residues involved in hydrogen bonding in the 562 gp120 complex. The V3 loop, bridging sheets, and CD4 are indicated by light green, cyan, and light pink, respectively. (B) Enlarged views of the binding surface between human CCR5 and the HIV-1 gp120 V3 loop. A ternary complex structure composed of 562 gp120, human CD4, and human CCR5 at 100 ns of MD simulation (Fig. 5A, upper left panel) was used to address molecular interactions. The model suggests that the V3 loop is stably embedded in the CCR5 N-terminal pocket via hydrophobic interactions between the ITI residues immediately upstream of the V3 loop tip (amino acid numbers 305 to 307 in 562 gp120) and two hydrophobic cores of CCR5 (green dotted circles). The interactions involve connections between V3 I305 and CCR5 F182/W190 and between V3 I307 and CCR5 C178/C101. Note that CCR5 I198 and V3 G310 are located near CCR5 Q194 around the CCR5 hydrophobic core and V3 T306 in the ITI motif, respectively. Views from two arbitrary angles are shown.

the V3 region acts as an electrostatic modulator of the global structure of gp120 outer domain (36). Together, these findings suggest that the long-range Coulomb interaction of V3 segment plays a key role in the species-specific growth of the 562 clone. Because the Coulomb interaction is known to affect most distantly among various noncovalent interactions, and because the V1/V2 and V3 regions are folded into proximity in the Env tertiary structure (7, 8, 27, 44), it is possible that a basic or an acidic substitution in V3 altered its potency of Coulomb interactions, influenced 3-D location of the V3 base, and thereby altered interactions between the V3 base and the bridging sheet (Fig. 9A). This possibility is consistent with the present observation that the G310R substitution somehow induces most prominently the augmentation of amino acid fluctuations around the V3 base with the human CD4-562 Env-gp120-human CCR5 complex (Fig. 5E). This in turn could influence conformation and structural dynamics of the bridging sheet for stable CD4 binding, as well as the binding mode of CD4 to gp120 (Fig. 6). Because the attractive forces via noncovalent interactions for the ligand binding reduce quickly in log order

by the distance extension, subtle changes in conformation around the CD4 binding surfaces could result in a marked reduction in the binding free energy (Fig. 6A, upper left panel). On the basis of the present findings of the experiments and MD simulations, we propose here that the V3 tip has a key function to allosterically regulate the CD4-gp120 interaction via influencing the Coulomb interaction network among the V3 base, the bridging sheet, and the CD4 apex.

Furthermore, the present study also provides new insights into regulation of the gp120-CCR5 interaction. The G310R substitution also affected the gp120-CCR5 interaction in a species-specific manner (Fig. 6A and 8). Our MD simulation suggests that the ITI triplet residues (amino acid positions 305 to 307 in 562 gp120) immediately upstream of the V3 tip generate attractive forces with hydrophobic cores in the CCR5 CRS2 region (Fig. 9B). Notably, the G310 residue in the V3 tip is placed at the face-to-face position against the T306 residue in the ITI triplet residues. Interestingly, the side chain of Y314 at the V3 loop is placed between the side chains of R310 and the ITI motif. Therefore, the G310R substitution that alters the size and chemical property of the side chain at position 310 would influence conformation and fluctuation of the ITI triplet residues via the Y314 residue. This in turn could influence the binding free energy (Fig. 6A), because the attractive force via hydrophobic interaction alters quickly in log order by distance extension or reduction.

The key role of the ITI motif in the gp120-CCR5 interaction is supported by the results obtained with CCR5 mutagenesis. Importantly, a single I198M substitution in the CRS2 region of CCR5 fairly restored the infectivity of the G310R mutant of 562 Env in human cells (Fig. 8), despite this residue not being directly involved in CCR5 binding (Fig. 2B). It should be noted that the I198 side chain is placed near the side chain of Q194 in the helix of the CCR5 CRS2 region (20) (Fig. 9B). Therefore, the I198M substitution could influence the conformation of the Q194 side chain and thereby that of the W190 side chain in the hydrophobic pocket in CRS2. This in turn could alter the shape of the hydrophobic pocket of CCR5 and thus the interactions between the ITI residues in the V3 tip and CCR5 CRS2. Furthermore, the conformational changes in the ITI region induced by the G310R and I198M substitutions could influence the fluctuation of the V3 base (Fig. 5E), possibly via conformational changes of the side chain at aromatic/hydrophobic residue Y314, and thereby alter the interaction between the V3 base and the bridging sheet of gp120 (Fig. 6). Thus, the results on the single substitutions at the V3 loop tip and CRS2 region of CCR5 consistently emphasize a key role of the ITI triplet residues in regulating the molecular interactions between gp120, CCR5, and CD4. Consistently, the effects of the G310R substitution in Env-gp120 on viral infectivity in macaque cells were dependent on the type of amino acid residue at position 306 in the ITI triplet (Fig. 10). It will be interesting to determine whether the G310R mutation has an impact on viral growth of HIV-1 strains that have Env sequences carrying the ITI residues, as observed for 562. Further study is required to clarify this issue, including the association of the ITI motif with interactions of Env-gp120 with CD4/CCR5.

The G310 residue at the V3 tip is highly conserved among HIV-1 strains in the world, whereas the corresponding residue of the HIV-2 and primate lentiviruses exhibit much greater variation (see the HIV Sequence Database, https://www.hiv.lanl.gov/content/sequence/HIV/mainpage.html). This and our present study suggest the regulatory role of the G310 residue has already been optimized in humans. In contrast, the ITI triplet residues show some variation among HIV-1 strains. This implies that the triplet motif is used for adaptive changes of HIV-1 to recover viral infectivity upon mutations at the V3 loop or other variable regions of gp120.

In summary, our study here uncovered biological and molecular features of a species-specific CD4/CCR5 interaction with Env-gp120 carrying a spontaneous mutation in the V3 tip. The obtained data suggest possible structural mechanisms by which gp120 undergoes the adaptive changes. The data further disclose the potential role of a network of intra- and intermolecular interactions for the balanced coordination of gp120

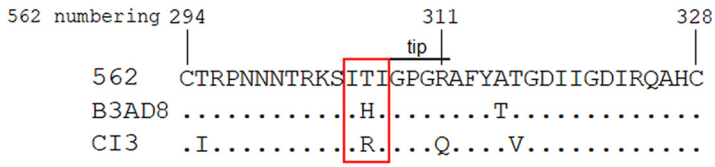

Virus clones	Growth in macaque cells
562	++
562-S304G	+++
562-G308V	+++
562-G310R	+++
B3AD8	++
B3AD8-G310R	+
CI3	++
CI3-G310R	–

FIG 10 Effect of G310R mutation on the growth ability of various virus clones. Amino acid sequences in the V3 loop regions of CCR5-tropic HIV-1mt clone 562 and the other two HIV-1mt clones designated B3AD8 and CI3 (63) are shown at the top. Dots indicate amino acids identical to those of 562. Note the boxed ITI motif. The growth abilities in macaque cells of the parental and mutant clones are qualitatively shown as follows: ++, parental clone; +++, grew better than each parental clone; +, grew more poorly than each parental clone; −, no detectable growth. For details, see Fig. 4 of this study and references 27 and 63.

binding affinities to CD4 and CCR5 proteins upon the switch of receptor tropism. The obtained information will accelerate our understanding of the regulation of the CD4-gp120-CCR5 ternary interactions, the structure-function relationship between distinct Env-gp120 sequences and various receptors, and the molecular steps critical for HIV-1 infection and adaptation.

MATERIALS AND METHODS

Cells. A CyM lymphocyte cell line, HSC-F (45), and a human lymphocyte cell line, MT4/R5 (26), were cultured and maintained in RPMI 1640 medium containing 10% heat-inactivated fetal bovine serum (for MT4/R5, 200 μg/ml of hygromycin B [Sigma-Aldrich] was added). Monolayer cell lines, HEK293T (ATCC CRL-1573) (46) and HeLa-derived luciferase reporter TZM-bl (47), were cultured and maintained in Eagle's minimal essential medium (MEM) containing 10% heat-inactivated fetal bovine serum (FBS). A HeLa-derived β-galactosidase reporter MAGI cell line (48) was cultured and maintained in MEM containing 10% heat-inactivated fetal bovine serum, 200 μg/ml of G418 (Sigma-Aldrich), and 100 μg/ml of hygromycin B.

Plasmid DNA. Proviral clones of HIV-1mt, 562, and its Env mutants were described previously (26, 27). New HIV-1 proviral clones were generated by introducing a fragment of the EcoRI site in *vpr* to the XhoI site in *nef* of 562 and that of its Env mutants (S304G, G308E, and G310R) into the corresponding sites of the HIV-1 NL4-3 clone (49), and the resultant clones were designated 562EX, 562EX-S304G, 562EX-G308E, and 562EX-G310R (Fig. 1). Mutants G308V, G310L, G310E, and G310K were newly constructed by site-directed mutagenesis using a parental clone 562, and the 562EX mutants were generated by recombination as described above. The human CCR5 expression vector, pCEP4-huCCR5, was a generous gift of Emi E. Nakayama (Osaka University, Japan). The human CCR5 mutants (K171R, I198M, and K171R/I198M) were generated by site-directed mutagenesis. To make the pCEP4-CyMCCR5 vector, the CCR5 coding sequence of CyM (CyMCCR5) was amplified by PCR using cDNA prepared from HSC-F cells, and the fragment was introduced into the pCEP4 vector by replacing the human CCR5 fragment of pCEP4-huCCR5. Amino acid sequences of human CCR5 and CyM CCR5 in the pCEP4 expression vector were identical to those of huCCR5 (GenBank accession number P51681) and CyMCCR5 (GenBank accession number P61814).

Viral infection experiments. Proviral clones were transfected into 293T cells by the calcium phosphate precipitation method as previously described (49, 50). Virus amounts were determined by virion-associated reverse transcriptase (RT) assays as previously described (50, 51). To assess viral growth potentials, equal amounts of virus samples were inoculated into CyM HSC-F cells, and the cells were cultured in the presence of IL-2 (Bio-Rad). For human MT4/R5 infection, the spin-infection method (52) was used. Culture supernatants were collected every 3 days postinfection, and virus replication was

monitored by RT assays. To determine viral infectivity, TZM-bl cells were infected with virus samples similarly as described previously (23). Evaluation of viral infectivity for MAGI cells transiently expressing various CCR5 proteins was performed as follows. MAGI cells were seeded into 96-well plates (2×10^4 cells per each well) and cultured overnight. Cells were then transfected with a series of pCEP4-CCR5 vectors with Lipofectamine 2000 (Thermo Fisher Scientific) and infected with equal amounts of virus samples (2.5×10^5 RT units for each of 562EX and 562EX-G310R) at 24 h posttransfection. On day 2 postinfection, cells were lysed for beta-galactosidase assays following the manufacturer's instructions (Beta-Glo assay system, Promega).

FACS analysis. Expression levels of cell surface CD4 and CCR5 were determined by FACS analysis as described previously (53). For monitoring CD4 expression, CyM HSC-F and human MT4/R5 cells were stained with fluorescein isothiocyanate (FITC) mouse anti-human CD4 clone L200 (catalog no. 550628; BD Biosciences). For monitoring transient CCR5 expression, MAGI cells transfected with various CCR5 expression vectors were stained with phycoerythrin (PE) mouse anti-human CD195 clone 3A9 (catalog no. 550632; BD Biosciences) at 24 h posttransfection. The stained cells were then analyzed by a BD FACSVerse flow cytometer and the BD FACSuite software (BD Biosciences).

Viral binding assays. To determine viral ability to attach to cell surface CD4, the binding assays using CyM HSC-F and human MT4/R5 cells were performed similarly as previously described (27). Input virus samples were prepared from 293T cells transfected with 562EX or 562EX-G310R, and those inactivated by incubation at 65°C for 45 min were used as negative controls. HSC-F and MT4/R5 cells (1×10^6) were incubated with viruses (1×10^6 RT units) at 4°C for 2 h, and cell lysates were prepared for the binding assays. For HSC-F cells, IL-2 was added into the reactions. The Gag-p24 levels in the cell lysates were quantified by the HIV-1 p24 antigen enzyme-linked immunosorbent assay kit (ZeptoMetrix Corporation). The binding capacity of each virus was calculated by subtracting the p24 value for negative (heat-inactivated) controls from that for test (virus-inoculated) samples.

Homology modeling of CD4-HIV-1 gp120-CCR5 complexes. The CD4-gp120-CCR5 complex models were constructed by homology modeling using the Molecular Operating Environment, MOE 2019.01 (Chemical Computing Group Inc., Montreal, QC, Canada), as described for the modeling of the gp120-CD4 complex (23, 27). The cryo-EM structure of the HIV-1 CD4-gp120-CCR5 complex at a resolution of 3.90 Å (PDB code 6MEO) (20) was used as the modeling template. HIV-1mt clone 562 or its gp120 V3 tip mutant (G310R or G308V) sequence was used for modeling of the gp120 region in the complex. The CD4 and CCR5 sequences of human or CyM were used for modeling of the CD4 and CCR5 region in the complex, respectively.

MD simulations. The CCR5 portions of the CD4-HIV-1 gp120-CCR5 complex models were embedded in a lipid bilayer. The lipid bilayer was composed of 1-palmitoyl-2-oleoyl-sn-glycero-3-phosphocholine (POPC), 1-palmitoyl-2-oleoyl-sn-glycero-3-phosphoethanolamine (POPE), and cholesterol at a ratio of 2:2:1 (2:2:1 POPC:POPE:cholesterol). The protein/lipid membrane complexes were constructed using the CHARMM-GUI Membrane Builder (54). All systems used the TIP3P water model (55) and had 0.15 M NaCl salt concentration added to the water layer. MD simulations were performed using the pmemd.cuda.MPI module in the Amber 16 program package (AMBER 2016, University of California, San Francisco), the amber ff14SB (56), and the lipid14 force field (57). Bond lengths involving hydrogen were constrained with SHAKE (58) and the time step for all MD simulations was set to 2 fs. A nonbonded cutoff of 10 Å was used. After performing heating calculations for 105 ps until 310 K using the NVT ensemble, we performed MD simulation with a barostat using the NPT ensemble at 1 bar and at 310 K for 10 ns in order to equilibrate the system's periodic boundary condition dimensions. Then, the production runs were executed using the NPT ensemble at 1 bar and at 310 K for 100 ns.

Calculation of binding free energy. The binding free energies of CD4 ($\Delta G_{bind.CD4,sol}$) or CCR5 ($\Delta G_{bind.CCR5,sol}$) to gp120 in solution were calculated from independent all-atom MD trajectories of CD4-gp120-CCR5 complexes from the last 5 ns (100 frames) after 100 ns of MD simulations. Calculation was done computationally using the MMPBSA.py tool (59) in the AmberTools16 (AMBER 2016, University of California, San Francisco). MMPBSA is a method to calculate the free energy of binding in solution in consideration of solvent-solvent interactions by incorporating information on the free energy of binding in a vacuum (59).

Calculation of RMSD and RMSF. RMSDs (60) between the heavy atoms of the initial complex structure and the structures at given time points of the MD simulation were calculated as described previously (27, 36) to monitor the overall structural changes during the MD simulations. The RMSD was calculated using the cpptraj module in the AmberTools 16. RMSFs of the Cα atoms of individual amino acids were calculated as described previously (27, 34–36) to quantify structural fluctuations of amino acid residues during the MD simulations. The 200 snapshots during 90 and 100 ns of the MD simulations were used to calculate RMSF using the ptraj module (60), a trajectory analysis tool in the AmberTools16. The average structures were used as reference structures for the RMSF calculation.

ACKNOWLEDGMENTS

This work was supported in part by a grant from the Takeda Science Foundation to M.N. and grants from the Japan Agency for Medical Research and Development (AMED) Research Program on HIV/AIDS (19fk0410027h0201 to M.N., 19fk0410027j0001 to O.K., and 19fk0410027j0401 to H.S.).

We thank Kazuko Yoshida for her editorial assistance.

The TZM-bl cells were obtained through the NIH AIDS Reagent Program, Division of AIDS, NIAID, NIH, from John C. Kappes, Xiaoyun Wu, and Tranzyme Inc. We appreciate the Support Center for Advanced Medical Sciences, Institute of Biomedical Sciences, Tokushima University Graduate School, for their experimental facilities and technical assistance.

REFERENCES

1. Chen B. 2019. Molecular mechanism of HIV-1 entry. Trends Microbiol 27:878–891. https://doi.org/10.1016/j.tim.2019.06.002.
2. Clapham PR, McKnight A. 2002. Cell surface receptors, virus entry and tropism of primate lentiviruses. J Gen Virol 83:1809–1829. https://doi.org/10.1099/0022-1317-83-8-1809.
3. Freed EO, Martin MA. 2013. Human immunodeficiency viruses: replication, p 1502–1560. In Knipe DM, Howley PM (ed), Fields virology, 6th ed, vol 2. Lippincott Williams & Wilkins, Philadelphia, PA.
4. Wilen CB, Tilton JC, Doms RW. 2012. HIV: cell binding and entry. Cold Spring Harb Perspect Med 2:a006866. https://doi.org/10.1101/cshperspect.a006866.
5. Brandenberg OF, Magnus C, Rusert P, Regoes RR, Trkola A. 2015. Different infectivity of HIV-1 strains is linked to number of envelope trimers required for entry. PLoS Pathog 11:e1004595. https://doi.org/10.1371/journal.ppat.1004595.
6. Zhu P, Liu J, Bess J, Jr., Chertova E, Lifson JD, Grisé H, Ofek GA, Taylor KA, Roux KH. 2006. Distribution and three-dimensional structure of AIDS virus envelope spikes. Nature 441:847–852. https://doi.org/10.1038/nature04817.
7. Julien JP, Cupo A, Sok D, Stanfield RL, Lyumkis D, Deller MC, Klasse PJ, Burton DR, Sanders RW, Moore JP, Ward AB, Wilson IA. 2013. Crystal structure of a soluble cleaved HIV-1 envelope trimer. Science 342:1477–1483. https://doi.org/10.1126/science.1245625.
8. Lyumkis D, Julien JP, de Val N, Cupo A, Potter CS, Klasse PJ, Burton DR, Sanders RW, Moore JP, Carragher B, Wilson IA, Ward AB. 2013. Cryo-EM structure of a fully glycosylated soluble cleaved HIV-1 envelope trimer. Science 342:1484–1490. https://doi.org/10.1126/science.1245627.
9. Freed EO, Myers DJ, Risser R. 1991. Identification of the principal neutralizing determinant of human immunodeficiency virus type 1 as a fusion domain. J Virol 65:190–194. https://doi.org/10.1128/JVI.65.1.190-194.1991.
10. Hoffman NG, Seillier-Moiseiwitsch F, Ahn J, Walker JM, Swanstrom R. 2002. Variability in the human immunodeficiency virus type 1 gp120 Env protein linked to phenotype-associated changes in the V3 loop. J Virol 76:3852–3864. https://doi.org/10.1128/JVI.76.8.3852-3864.2002.
11. Pastore C, Nedellec R, Ramos A, Pontow S, Ratner L, Mosier DE. 2006. Human immunodeficiency virus type 1 coreceptor switching: V1/V2 gain-of-fitness mutations compensate for V3 loss-of-fitness mutations. J Virol 80:750–758. https://doi.org/10.1128/JVI.80.2.750-758.2006.
12. Roche M, Jakobsen MR, Sterjovski J, Ellett A, Posta F, Lee B, Jubb B, Westby M, Lewin SR, Ramsland PA, Churchill MJ, Gorry PR. 2011. HIV-1 escape from the CCR5 antagonist maraviroc associated with an altered and less-efficient mechanism of gp120-CCR5 engagement that attenuates macrophage tropism. J Virol 85:4330–4342. https://doi.org/10.1128/JVI.00106-11.
13. Willey RL, Theodore TS, Martin MA. 1994. Amino acid substitutions in the human immunodeficiency virus type 1 gp120 V3 loop that change viral tropism also alter physical and functional properties of the virion envelope. J Virol 68:4409–4419. https://doi.org/10.1128/JVI.68.7.4409-4419.1994.
14. Brelot A, Chakrabarti LA. 2018. CCR5 revisited: how mechanisms of HIV entry govern AIDS pathogenesis. J Mol Biol 430:2557–2589. https://doi.org/10.1016/j.jmb.2018.06.027.
15. Tan Q, Zhu Y, Li J, Chen Z, Han GW, Kufareva I, Li T, Ma L, Fenalti G, Li J, Zhang W, Xie X, Yang H, Jiang H, Cherezov V, Liu H, Stevens RC, Zhao Q, Wu B. 2013. Structure of the CCR5 chemokine receptor-HIV entry inhibitor maraviroc complex. Science 341:1387–1390. https://doi.org/10.1126/science.1241475.
16. Doranz BJ, Lu ZH, Rucker J, Zhang TY, Sharron M, Cen YH, Wang ZX, Guo HH, Du JG, Accavitti MA, Doms RW, Peiper SC. 1997. Two distinct CCR5 domains can mediate coreceptor usage by human immunodeficiency virus type 1. J Virol 71:6305–6314. https://doi.org/10.1128/JVI.71.9.6305-6314.1997.
17. Huang CC, Lam SN, Acharya P, Tang M, Xiang SH, Hussan SS, Stanfield RL, Robinson J, Sodroski J, Wilson IA, Wyatt R, Bewley CA, Kwong PD. 2007. Structures of the CCR5 N terminus and of a tyrosine-sulfated antibody with HIV-1 gp120 and CD4. Science 317:1930–1934. https://doi.org/10.1126/science.1145373.
18. Tamamis P, Floudas CA. 2014. Molecular recognition of CCR5 by an HIV-1 gp120 V3 loop. PLoS One 9:e95767. https://doi.org/10.1371/journal.pone.0095767.
19. Zheng Y, Han GW, Abagyan R, Wu B, Stevens RC, Cherezov V, Kufareva I, Handel TM. 2017. Structure of CC chemokine receptor 5 with a potent chemokine antagonist reveals mechanisms of chemokine recognition and molecular mimicry by HIV. Immunity 46:1005–1017. https://doi.org/10.1016/j.immuni.2017.05.002.
20. Shaik MM, Peng H, Lu J, Rits-Volloch S, Xu C, Liao M, Chen B. 2019. Structural basis of coreceptor recognition by HIV-1 envelope spike. Nature 565:318–323. https://doi.org/10.1038/s41586-018-0804-9.
21. Boyd DF, Peterson D, Haggarty BS, Jordan AP, Hogan MJ, Goo L, Hoxie JA, Overbaugh J. 2015. Mutations in HIV-1 envelope that enhance entry with the macaque CD4 receptor alter antibody recognition by disrupting quaternary interactions within the trimer. J Virol 89:894–907. https://doi.org/10.1128/JVI.02680-14.
22. Del Prete GQ, Keele BF, Fode J, Thummar K, Swanstrom AE, Rodriguez A, Raymond A, Estes JD, LaBranche CC, Montefiori DC, KewalRamani VN, Lifson JD, Bieniasz PD, Hatziioannou T. 2017. A single gp120 residue can affect HIV-1 tropism in macaques. PLoS Pathog 13:e1006572. https://doi.org/10.1371/journal.ppat.1006572.
23. Doi N, Yokoyama M, Koma T, Kotani O, Sato H, Adachi A, Nomaguchi M. 2019. Concomitant enhancement of HIV-1 replication potential and neutralization-resistance in concert with three adaptive mutations in Env V1/C2/C4 domains. Front Microbiol 10:2. https://doi.org/10.3389/fmicb.2019.00002.
24. Humes D, Emery S, Laws E, Overbaugh J. 2012. A species-specific amino acid difference in the macaque CD4 receptor restricts replication by global circulating HIV-1 variants representing viruses from recent infection. J Virol 86:12472–12483. https://doi.org/10.1128/JVI.02176-12.
25. Humes D, Overbaugh J. 2011. Adaptation of subtype A human immunodeficiency virus type 1 envelope to pig-tailed macaque cells. J Virol 85:4409–4420. https://doi.org/10.1128/JVI.02244-10.
26. Nomaguchi M, Doi N, Fujiwara S, Saito A, Akari H, Nakayama EE, Shioda T, Yokoyama M, Sato H, Adachi A. 2013. Systemic biological analysis of the mutations in two distinct HIV-1mt genomes occurred during replication in macaque cells. Microbes Infect 15:319–328. https://doi.org/10.1016/j.micinf.2013.01.005.
27. Yokoyama M, Nomaguchi M, Doi N, Kanda T, Adachi A, Sato H. 2016. *In silico* analysis of HIV-1 Env-gp120 reveals structural bases for viral adaptation in growth-restrictive cells. Front Microbiol 7:110. https://doi.org/10.3389/fmicb.2016.00110.
28. Xue B, Mizianty MJ, Kurgan L, Uversky VN. 2012. Protein intrinsic disorder as a flexible armor and a weapon of HIV-1. Cell Mol Life Sci 69:1211–1259. https://doi.org/10.1007/s00018-011-0859-3.
29. Zolla-Pazner S, Cardozo T. 2010. Structure-function relationships of HIV-1 envelope sequence-variable regions refocus vaccine design. Nat Rev Immunol 10:527–535. https://doi.org/10.1038/nri2801.
30. Nomaguchi M, Doi N, Kamada K, Adachi A. 2008. Species barrier of HIV-1 and its jumping by virus engineering. Rev Med Virol 18:261–275. https://doi.org/10.1002/rmv.576.
31. Nomaguchi M, Yokoyama M, Kono K, Nakayama EE, Shioda T, Saito A, Akari H, Yasutomi Y, Matano T, Sato H, Adachi A. 2013. Gag-CA Q110D mutation elicits TRIM5-independent enhancement of HIV-1mt replication in macaque cells. Microbes Infect 15:56–65. https://doi.org/10.1016/j.micinf.2012.10.013.
32. Selyutina A, Persaud M, Simons LM, Bulnes-Ramos A, Buffone C, Martinez-Lopez A, Scoca V, Di Nunzio F, Hiatt J, Marson A, Krogan NJ, Hultquist JF, Diaz-Griffero F. 2020. Cyclophilin A prevents HIV-1 restriction in lymphocytes by blocking human TRIM5α binding to the viral core. Cell Rep 30:3766–3777. https://doi.org/10.1016/j.celrep.2020.02.100.

33. Schaller T, Ocwieja KE, Rasaiyaah J, Price AJ, Brady TL, Roth SL, Hué S, Fletcher AJ, Lee K, KewalRamani VN, Noursadeghi M, Jenner RG, James LC, Bushman FD, Towers GJ. 2011. HIV-1 capsid-cyclophilin interactions determine nuclear import pathway, integration targeting and replication efficiency. PLoS Pathog 7:e1002439. https://doi.org/10.1371/journal.ppat.1002439.
34. Hikichi Y, Yokoyama M, Takemura T, Fujino M, Kumakura S, Maeda Y, Yamamoto N, Sato H, Matano T, Murakami T. 2016. Increased HIV-1 sensitivity to neutralizing antibodies by mutations in the Env V3-coding region for resistance to CXCR4 antagonists. J Gen Virol 97:2427–2440. https://doi.org/10.1099/jgv.0.000536.
35. Kuwata T, Takaki K, Yoshimura K, Enomoto I, Wu F, Ourmanov I, Hirsch VM, Yokoyama M, Sato H, Matsushita S. 2013. Conformational epitope consisting of the V3 and V4 loops as a target for potent and broad neutralization of simian immunodeficiency viruses. J Virol 87:5424–5436. https://doi.org/10.1128/JVI.00201-13.
36. Yokoyama M, Naganawa S, Yoshimura K, Matsushita S, Sato H. 2012. Structural dynamics of HIV-1 envelope gp120 outer domain with V3 loop. PLoS One 7:e37530. https://doi.org/10.1371/journal.pone.0037530.
37. Kwong PD, Wyatt R, Robinson J, Sweet RW, Sodroski J, Hendrickson WA. 1998. Structure of an HIV gp120 envelope glycoprotein in complex with the CD4 receptor and a neutralizing human antibody. Nature 393:648–659. https://doi.org/10.1038/31405.
38. Lau G, Labrecque J, Metz M, Vaz R, Fricker SP. 2015. Specificity for a CCR5 inhibitor is conferred by a single amino acid residue: role of Ile198. J Biol Chem 290:11041–11051. https://doi.org/10.1074/jbc.M115.640169.
39. Colin P, Zhou Z, Staropoli I, Garcia-Perez J, Gasser R, Armani-Tourret M, Benureau Y, Gonzalez N, Jin J, Connell BJ, Raymond S, Delobel P, Izopet J, Lortat-Jacob H, Alcami J, Arenzana-Seisdedos F, Brelot A, Lagane B. 2018. CCR5 structural plasticity shapes HIV-1 phenotypic properties. PLoS Pathog 14:e1007432. https://doi.org/10.1371/journal.ppat.1007432.
40. Kowalski M, Potz J, Basiripour L, Dorfman T, Goh WC, Terwilliger E, Dayton A, Rosen C, Haseltine W, Sodroski J. 1987. Functional regions of the envelope glycoprotein of human immunodeficiency virus type 1. Science 237:1351–1355. https://doi.org/10.1126/science.3629244.
41. Lasky LA, Nakamura G, Smith DH, Fennie C, Shimasaki C, Patzer E, Berman P, Gregory T, Capon DJ. 1987. Delineation of a region of the human immunodeficiency virus type 1 gp120 glycoprotein critical for interaction with the CD4 receptor. Cell 50:975–985. https://doi.org/10.1016/0092-8674(87)90524-1.
42. Olshevsky U, Helseth E, Furman C, Li J, Haseltine W, Sodroski J. 1990. Identification of individual human immunodeficiency virus type 1 gp120 amino acids important for CD4 receptor binding. J Virol 64:5701–5707. https://doi.org/10.1128/JVI.64.12.5701-5707.1990.
43. Wang H, Cohen AA, Galimidi RP, Gristick HB, Jensen GJ, Bjorkman PJ. 2016. Cryo-EM structure of a CD4-bound open HIV-1 envelope trimer reveals structural rearrangements of the gp120 V1V2 loop. Proc Natl Acad Sci U S A 113:E7151–E7158. https://doi.org/10.1073/pnas.1615939113.
44. Liu J, Bartesaghi A, Borgnia MJ, Sapiro G, Subramaniam S. 2008. Molecular architecture of native HIV-1 gp120 trimers. Nature 455:109–113. https://doi.org/10.1038/nature07159.
45. Akari H, Fukumori T, Iida S, Adachi A. 1999. Induction of apoptosis in Herpesvirus saimiri-immortalized T lymphocytes by blocking interaction of CD28 with CD80/CD86. Biochem Biophys Res Commun 263:352–356. https://doi.org/10.1006/bbrc.1999.1364.
46. Lebkowski JS, Clancy S, Calos MP. 1985. Simian virus 40 replication in adenovirus-transformed human cells antagonizes gene expression. Nature 317:169–171. https://doi.org/10.1038/317169a0.
47. Platt EJ, Bilska M, Kozak SL, Kabat D, Montefiori DC. 2009. Evidence that ecotropic murine leukemia virus contamination in TZM-bl cells does not affect the outcome of neutralizing antibody assays with human immunodeficiency virus type 1. J Virol 83:8289–8292. https://doi.org/10.1128/JVI.00709-09.
48. Kimpton J, Emerman M. 1992. Detection of replication-competent and pseudotyped human immunodeficiency virus with a sensitive cell line on the basis of activation of an integrated beta-galactosidase gene. J Virol 66:2232–2239. https://doi.org/10.1128/JVI.66.4.2232-2239.1992.
49. Adachi A, Gendelman HE, Koenig S, Folks T, Willey R, Rabson A, Martin MA. 1986. Production of acquired immunodeficiency syndrome-associated retrovirus in human and nonhuman cells transfected with an infectious molecular clone. J Virol 59:284–291. https://doi.org/10.1128/JVI.59.2.284-291.1986.
50. Nomaguchi M, Yokoyama M, Kono K, Nakayama EE, Shioda T, Doi N, Fujiwara S, Saito A, Akari H, Miyakawa K, Ryo A, Ode H, Iwatani Y, Miura T, Igarashi T, Sato H, Adachi A. 2013. Generation of rhesus macaque-tropic HIV-1 clones that are resistant to major anti-HIV-1 restriction factors. J Virol 87:11447–11461. https://doi.org/10.1128/JVI.01549-13.
51. Willey RL, Smith DH, Lasky LA, Theodore TS, Earl PL, Moss B, Capon DJ, Martin MA. 1988. In vitro mutagenesis identifies a region within the envelope gene of the human immunodeficiency virus that is critical for infectivity. J Virol 62:139–147. https://doi.org/10.1128/JVI.62.1.139-147.1988.
52. O'Doherty U, Swiggard WJ, Malim MH. 2000. Human immunodeficiency virus type 1 spinoculation enhances infection through virus binding. J Virol 74:10074–10080. https://doi.org/10.1128/JVI.74.21.10074-10080.2000.
53. Nomaguchi M, Doi N, Fujiwara S, Fujita M, Adachi A. 2010. Site-directed mutagenesis of HIV-1 *vpu* gene demonstrates two clusters of replication-defective mutants with distinct ability to down-modulate cell surface CD4 and tetherin. Front Microbiol 1:116. https://doi.org/10.3389/fmicb.2010.00116.
54. Jo S, Lim JB, Klauda JB, Im W. 2009. CHARMM-GUI Membrane Builder for mixed bilayers and its application to yeast membranes. Biophys J 97:50–58. https://doi.org/10.1016/j.bpj.2009.04.013.
55. Jorgensen WL, Chandrasekhar J, Madura JD, Impey RW, Klein ML. 1983. Comparison of simple potential functions for simulating liquid water. J Chem Phys 79:926–935. https://doi.org/10.1063/1.445869.
56. Maier JA, Martinez C, Kasavajhala K, Wickstrom L, Hauser KE, Simmerling C. 2015. ff14SB: improving the accuracy of protein side chain and backbone parameters from ff99SB. J Chem Theory Comput 11:3696–3713. https://doi.org/10.1021/acs.jctc.5b00255.
57. Dickson CJ, Madej BD, Skjevik AA, Betz RM, Teigen K, Gould IR, Walker RC. 2014. Lipid14: the Amber lipid force field. J Chem Theory Comput 10:865–879. https://doi.org/10.1021/ct4010307.
58. Ryckaert JP, Ciccotti G, Berendsen HJC. 1977. Numerical integration of the cartesian equations of motion of a system with constraints: molecular dynamics of n-alkanes. J Comput Phys 23:327–341. https://doi.org/10.1016/0021-9991(77)90098-5.
59. Miller BR, 3rd, McGee TD, Jr., Swails JM, Homeyer N, Gohlke H, Roitberg AE. 2012. MMPBSA.py: an efficient program for end-state free energy calculations. J Chem Theory Comput 8:3314–3321. https://doi.org/10.1021/ct300418h.
60. Case DA, Cheatham TE, 3rd, Darden T, Gohlke H, Luo R, Merz KM, Jr., Onufriev A, Simmerling C, Wang B, Woods RJ. 2005. The Amber biomolecular simulation programs. J Comput Chem 26:1668–1688. https://doi.org/10.1002/jcc.20290.
61. Shibata R, Kawamura M, Sakai H, Hayami M, Ishimoto A, Adachi A. 1991. Generation of a chimeric human and simian immunodeficiency virus infectious to monkey peripheral blood mononuclear cells. J Virol 65:3514–3520. https://doi.org/10.1128/JVI.65.7.3514-3520.1991.
62. Kawamura M, Ishizaki T, Ishimoto A, Shioda T, Kitamura T, Adachi A. 1994. Growth ability of human immunodeficiency virus type 1 auxiliary gene mutants in primary blood macrophage cultures. J Gen Virol 75:2427–2431. https://doi.org/10.1099/0022-1317-75-9-2427.
63. Doi N, Sakai Y, Adachi A, Nomaguchi M. 2017. Generation and characterization of new CCR5-tropic HIV-1rmt clones. J Med Invest 64:272–279. https://doi.org/10.2152/jmi.64.272.